Influence of Steric and Electronic Perturbations on the Polymerization Activities of α-Iminocarboxamide Nickel Complexes

Jason D. Azoulay, Koji Itigaki, Guang Wu, and Guillermo C. Bazan*

Mitsubishi Chemical Center for Advanced Materials, Institute for Polymer and Organic Solids, Departments of Chemistry & Biochemistry and Materials, University of California, Santa Barbara, California 93106

Received January 10, 2008

A series of *N,O*-bound, neutral nickel complexes containing α-iminocarboxamide, η^1-CH_2Ph, and PMe_3 ligands were synthesized to examine the effect of steric and electronic variations at the site adjacent to the imine functionality. These complexes were subsequently activated with $Ni(COD)_2$ for use in ethylene homopolymerization and ethylene/norbornene acetate (NBA) copolymerization reactions. As the bulk of the substituents is increased, one observes a progressive decrease in the rate of ring rotation, a more crowded coordination sphere around nickel, increased monomer consumption activity, and higher molecular weights of the products. Copolymerization reactions showed that the increased crowding around nickel decreases the reactivity of NBA relative to ethylene. As electron density is removed from the metal center, the catalytic species become more active toward ethylene and are more prone to interact with the functionality on NBA.

Introduction

Polyolefins are commodity materials with major economic implications. Metal-mediated polymerizations that serve in this context continue to be an active research area in academic and industrial laboratories.[1] Late transition metal initiators for olefin polymerization and oligomerization are of particular interest due to their lower oxophilicity and greater functional group tolerance, relative to their early transition metal counterparts.[2] Nickel-based catalysts have been shown to participate in chain walking reactions,[3] tolerate polar functionalities,[4] and have even been used in water.[5] These catalytic properties are significant for developing materials with unique properties.[1]

Activation of [*N*-(2,6-diisopropylphenyl)-2-(2,6-diisopropylphenylimino)propanimidato-κ^2N,O]Ni(η^1-CH_2Ph)(PMe_3), **1**, by $Ni(COD)_2$ generates an active site capable of copolymerizing ethylene and 5-norbornen-2-yl acetate (NBA) in a quasi-living fashion.[6] The time-dependent growth of M_n and relatively narrow molecular weight distributions (PDIs) have allowed for the preparation of complex polymeric architectures. Block copolymers containing segments of random sequences of ethylene and NBA with different molar compositions[7] show microphase separation and have the potential to reduce the interfacial energy between polyolefins and polar plastics. More recently, tapered tetrablock copolymers,[8] composed of alternating amorphous and semicrystalline block segments, have been synthesized and possess elastomeric properties.The basic structural framework of α-iminocarboxamide ligands is shown in Figure 1. Variations studied thus far incorporate a methyl group adjacent to the imine functionality. Changes in Ar_1 and Ar_2 modify the binding preferences to the [Ni(CH_2Ph)PMe_3] fragment. When the combined steric bulk in Ar_1 and Ar_2 is sufficiently large, the *N,O*-binding mode is observed. Reduction

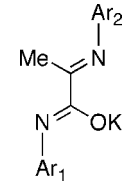

Figure 1. General structure of α-iminocarboxamidate ligands.

* Corresponding author. Fax: +1 805 893 4120. Tel: +1 805 893 5538. E-mail: bazan@chem.ucsb.edu.

(1) (a) Rieger, B.; Baugh, L.; Striegler, S.; Kacker, S. *Late Transition Metal Polymerization Catalysis*; John Wiley & Sons: New York, 2003. (b) Blom, R.; Follestad, A.; Rytter, E.; Tilset, M.; Ystenes, M. *Organometallic Catalysts and Olefin Polymerization: Catalysts for a New Millennium*; Springer-Verlag: Berlin, Germany, 2001. (c) Galli, P.; Vecellio, G. *J. Polym. Sci. Part A: Polym. Chem.* **2004**, *42*, 396. (d) Keim, W.; Kowalt, F. H.; Goddard, R.; Kruger, C. *Angew. Chem., Int. Ed.* **1978**, *17*, 466. (e) Bonnet, M. C.; Dahan, F.; Ecke, A.; Keim, W.; Schultz, R. P.; Tkatchenko, I. *Chem. Commun.* **1994**, 615 For relevant reviews see: (f) Ittel, S. D.; Johnson, L. K.; Brookhart, M. *Chem. Rev.* **2000**, *100*, 1169. (g) Boffa, L. S.; Novak, B. M. *Chem. Rev.* **2000**, *100*, 1479. (h) Yanjarappa, M. J.; Sivaram, S. *Prog. Polym. Sci.* **2002**, *27*, 1347. (i) Mecking, S.; Held, A.; Bauers, F. M. *Angew. Chem., Int. Ed.* **2002**, *41*, 544. (j) Gibson, V. C.; Spitzmesser, S. K. *Chem. Rev.* **2003**, *103*, 283. (k) Mecking, S. *Coord. Chem. Rev.* **2000**, *203*, 325. (l) Domski, G. J.; Rose, J. M.; Goates, G. W.; Bolig, A. D.; Brookhart, M. *Prog. Polym. Sci.* **2007**, *32*, 30.

(2) (a) Johnson, L. K.; Mecking, S.; Brookhart, M. *J. Am. Chem. Soc.* **1996**, *118*, 267. (b) Mecking, S.; Johnson, L. K.; Wang, L.; Brookhart, M. *J. Am. Chem. Soc.* **1998**, *120*, 888. (c) Kuhn, P.; Semeril, D.; Matt, D.; Chetuchi, M. J.; Lutz, P. *Dalton Trans.* **2007**, 515.

(3) Leatherman, M. D.; Svedja, S. A.; Johnson, L. K.; Brookhart, M. *J. Am. Chem. Soc.* **2003**, *125*, 3068.

(4) (a) Younkin, T. R.; Conor, E. F.; Henderson, J. I.; Friedrich, S. K.; Grubbs, R. H.; Bansleben, D. A. *Science* **2000**, *287*, 460. (b) Connor, E. F.; Younkin, T. R.; Henderson, J. I.; Hwang, S.; Grubbs, R. H.; Roberts, W. P.; Litzau, J. J. *J. Polym. Sci.: Part A: Polym. Chem.* **2002**, *40*, 2842.

(5) (a) Held, A.; Bauers, F. M.; Mecking, S.; Friedrich, S. K *Chem. Commun.* **2000**, 301. (b) Bauers, F. M.; Mecking, S. *Macromolecules* **2001**, *34*, 1165. (c) Korthals, B.; Schnetmann, I. G.; Mecking, S. *Organometallics* **2007**, *26*, 1311.

(6) Diamanti, S. J.; Ghosh, P.; Shimizu, F.; Bazan, G. C. *Macromolecules* **2003**, *36*, 9731.

(7) (a) Diamanti, S. J.; Khanna, V.; Hotta, A.; Yamakawa, D.; Shimizu, F.; Kramer, E. J.; Fredrickson, G. H.; Bazan, G. C. *J. Am. Chem. Soc.* **2004**, *126*, 10528. (b) Diamanti, S. J.; Khanna, V.; Hotta, A.; Coffin, R. C.; Yamakawa, D.; Kramer, E. J.; Fredrickson, G. H.; Bazan, G. C. *Macromolecules* **2006**, *39*, 3270.

(8) Coffin, R. C.; Diamanti, S. J.; Hotta, A.; Khanna, V.; Kramer, E. J.; Frederickson, G. H.; Bazan, G. C. *Chem. Commun.* **2007**, 3550.

10.1021/om8000263 CCC: $40.75
Publication on Web 04/16/2008

of the steric interference gives rise to complexes that take advantage of the electronically preferred *N,N*-binding geometry. Only *N,O*-bound complexes give rise to useful catalytic species in the presence of $Ni(COD)_2$ or to single-component catalysts.[9] The preference of "catalytic species" over "initiating species" has been discussed previously.[11]

In this contribution, we provide an improved synthetic route to α-iminocarboxamide ligands, which allows for the incorporation of substituents that were designed to probe steric and electronic perturbations at the site adjacent to the imine group, i.e., replacement of Me in Figure 1. More significantly, we demonstrate that the resulting complexes provide catalysts with improved performance in terms of elevated activities and narrower molecular weight distributions. These reaction features allow for better control over the final polymer product in both homopolymerization and copolymerization reactions

Results and Discussion

Synthesis and Characterization of α-Iminocarboxamide Nickel Complexes. The synthesis of α-iminocarboxamide ligands typically begins by the reaction of pyruvic acid, or the corresponding sodium salt, with oxalyl chloride, to generate the acid chloride in situ. Reaction with anilines at the acid chloride site is promoted by the addition of an equivalent of triethylamine. 2,6-Diisopropylaryl substituents were of interest due to their known stabilization of reactive nickel centers and tendency to increase the molecular weight of the polyethylene product.[10] The condensation of a second equivalent of 2,6-diisopropylaniline typically takes place by heating in the presence of catalytic acid. Using this approach, one obtains conversions of >95% and ~70% when R = Et and CH_2CHMe_2, respectively, and fails in the presence of other, more hindered substrates. A new synthetic procedure thus had to be established to systematically evaluate variations in the backbone size.

An improved method for the condensation of anilines with pyruvamides was found that utilizes $TiCl_4$[11] and triethylamine in toluene and provides the desired α-iminocarboxamide ligands in >90% conversion. In this reaction, a solution of $TiCl_4$ is added to a solution of 2,6-diisopropylaniline and excess triethylamine at low temperature. The pyruvamide is subsequently added and the reaction mixture is allowed to stir and warm to room temperature. Reaction times are substrate dependent. The overall process is illustrated in Scheme 1. Conversions of >95% were obtained when R = Et, CH_2CHMe_2, Ph, *p*-CF_3-Ph, and *p*-OCH_3-Ph. For the bulkiest substrate, R = $CHMe_2$, the reaction mixture required heating to 85 °C, and approximately 90% of the substrate was converted to the desired product.

Deprotonation using KH in THF provided the potassium salts of the ligands, which were subsequently reacted with $Ni(\eta^1\text{-}CH_2Ph)Cl(PMe_3)_2$ in toluene at room temperature for 2.5 h.[12] The products of these reactions contain nickel ligated by α-iminocarboxamide, η^1-CH_2Ph, and PMe_3 ligands as determined by ^1H and ^{13}C NMR spectroscopies. A single isomer is observed in all cases with respect to the PMe_3 orientation relative to the imine nitrogen. From the ^{31}P NMR signals, which fall in the range $\delta = -7.85$ to -8.06 ppm for all products, it is possible to determine that the α-iminocarboxamide fragment is coordinated in an *N,O*-fashion.[13] For comparison, *N,N*-bound complexes exhibit ^{31}P NMR signals ranging from -20.0 to -25.0 ppm, depending on the ligand framework. These data are consistent with the formation of [*N*-(2,6-diisopropylphenyl)-2-(2,6-diisopropylphenylimino)butanamidato-κ^2N,O](η^1-CH_2Ph)(PMe_3)nickel (**2**, R = Et), [*N*-(2,6-diisopropylphenyl)-2-(2,6-diisopropylphenylimino)-4-methylpentanamidato-κ^2N,O](η^1-CH_2Ph)(PMe_3)nickel (**3**, R = CH_2CHMe_2), [*N*-(2,6-diisopropylphenyl)-2-(2,6-diisopropylphenylimino)-3-methylbutanamidato-κ^2N,O](η^1-CH_2Ph)(PMe_3)nickel (**4**, R = $CHMe_2$), [*N*-(2,6-diisopropylphenyl)-2-(2,6-diisopropylphenylimino)-2-phenylethanamidato-κ^2N,O](η^1-CH_2Ph)(PMe_3)nickel (**5**, R = Ph), [*N*-(2,6-diisopropylphenyl)-2-(2,6-diisopropylphenylimino)-2-(4-(trifluoromethyl)phenyl)ethanamidato-κ^2N,O](η^1-CH_2Ph)(PMe_3)-nickel (**6**, R = *p*-CF_3-Ph), and [*N*-(2,6-diisopropylphenyl)-2-(2,6-diisopropylphenylimino)-2-(4-methoxyphenyl)ethanamidato-κ^2N,O](η^1-CH_2Ph)(PMe_3)nickel (**7**, R = *p*-OCH_3-Ph). The presence of a trifluoromethyl substituent in compound **6** was verified by a singlet ($\delta = -0.26$ ppm) in the ^{19}F NMR spectrum. The compositions of **2**–**7** were verified by elemental analysis.

Scheme 1. Synthetic Approach to Substituted α-Iminocarboxamide Ligands[a]

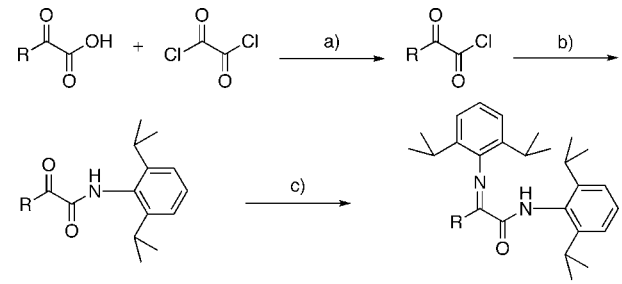

[a] (a) Triethylamine, toluene (0 °C to RT); (b) 2,6-diisopropylaniline, triethylamine, toluene, RT; (c) 2,6-diisopropylaniline, $TiCl_4$, triethylamine, toluene, 0−85 °C (depending on substrate).

Figure 2 highlights the ^1H NMR spectra at room temperature of compounds **1**–**4** in the 0.4 to 1.8 ppm range. This series can be used to probe steric effects on the properties of the complexes. Of particular interest in Figure 2 are the methyl signals arising from the isopropyl groups on the aryl ring bound to the carboxamide nitrogen, i.e., Ar_1 in Figure 1.[9,13] For all spectra, the isopropyl groups on Ar_2 provide for two doublets; they do not average by rotation of the aryl ring within the time scale of the NMR experiment. In the case of **1**, a broad doublet is observed, centered around $\delta = 1.58$ ppm. For **2**, the signal broadens, and in the case of **3**, two broad signals at $\delta = 1.77$–1.62 ppm and $\delta = 1.62$–1.54 ppm are observed. The spectrum of **4** shows two resolved doublets at $\delta = 1.73$ ppm and $\delta = 1.63$ ppm. These data are consistent with a progressive decrease in the rate of ring rotation with increasing size at the R position. This trend also implies that $CHMe_2$ is bulkier than CH_2CHMe_2. For completeness, we point out that compounds **5**–**7**, which incorporate differences in both the steric and electronic properties of the ligand, exhibit ^1H NMR spectra similar to the spectrum of compound **2**.

Crystallization from pentane at −35 °C provided single crystals suitable for X-ray diffraction studies of compounds **2**–**5**.

(9) (a) Rojas, R. S.; Wasilke, J. C.; Wu, G.; Ziller, J. W.; Bazan, G. C. *Organometallics* **2005**, *24*, 5644. (b) Rojas, R. S.; Galland, G. B.; Wu, G.; Bazan, G. C. *Organometallics* **2007**, *26*, 5339.

(10) (a) Johnsohn, L. K.; Killian, C. M.; Brookhart, M. *J. Am. Chem. Soc.* **1995**, *117*, 6414. (b) Svedja, S. A.; Johnsohn, L. K.; Brookhart, M. *J. Am. Chem. Soc.* **1999**, *121*, 10634.

(11) Carlson, R.; Larsson, U.; Hansson, L. *Acta Chem. Scand.* **1992**, *46*, 1211.

(12) Carmona, E.; Paneque, M.; Poveda, M. L. *Polyhedron* **1989**, *8*, 285.

(13) Lee, B. Y.; Bazan, G. C.; Vela, J.; Komon, Z. J.; Bu, X. *J. Am. Chem. Soc.* **2001**, *123*, 5352.

Scheme 2. Synthesis of 2–7 (reactions were carried out in toluene at RT for 2.5 h)

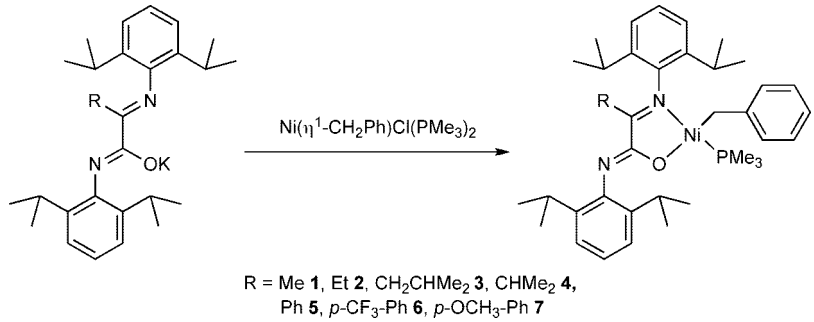

R = Me **1**, Et **2**, CH_2CHMe_2 **3**, $CHMe_2$ **4**, Ph **5**, *p*-CF_3-Ph **6**, *p*-OCH_3-Ph **7**

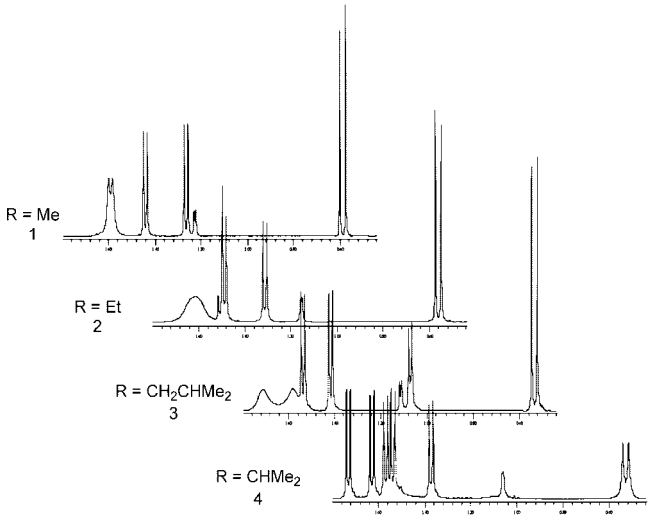

Figure 2. ^{1}H NMR spectra of **1**–**4** in the 0.4–1.8 ppm range at 25 °C illustrating a progressive decrease in the rate of ring rotation with increasing size at the R position.

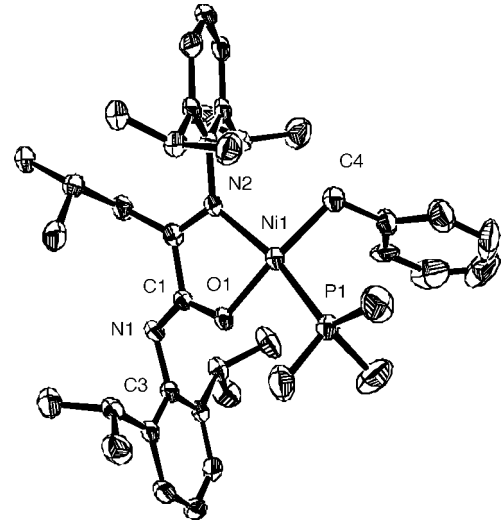

Figure 4. ORTEP drawing of **3** (R = CH_2CHMe_2) at the 50% probability level. Hydrogen atoms are omitted for clarity.

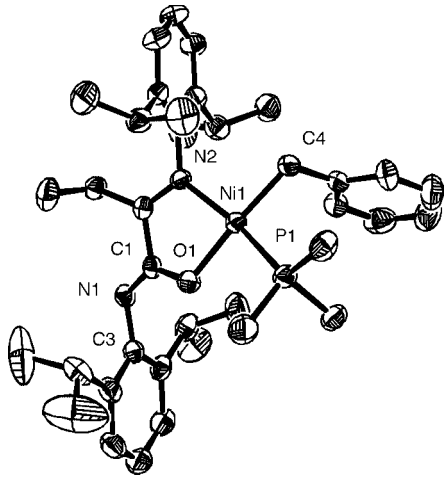

Figure 3. ORTEP drawing of **2** (R = Et) at the 50% probability level. Hydrogen atoms are omitted for clarity.

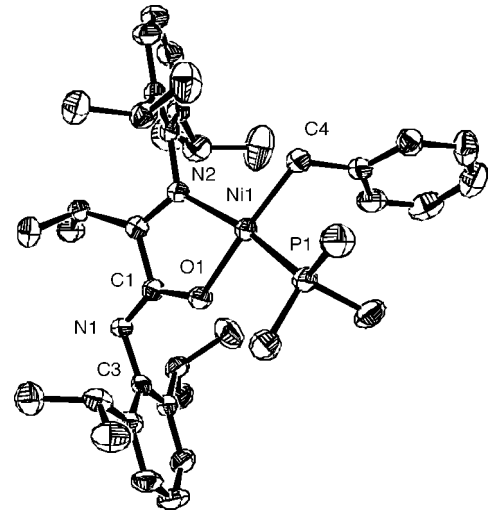

Figure 5. ORTEP drawing of **4** (R = $CHMe_2$) at the 50% probability level. Hydrogen atoms are omitted for clarity.

Repeated efforts to obtain suitable crystals were not successful for **6** and **7**. Results from these studies, provided in Figures 3–6, confirm the structures of compounds **2**–**5** as shown in Scheme 2. Table 1 provides a summary of the metrical data, together with previously attained data for compound **1** for comparison purposes.[13] As a result of the increased bulk, the coordination sphere around nickel is more crowded in **2**, **3**, and **4**, relative to **1**. Larger distortions from square-planar geometry are evident, as shown by the angle between the N(2)−Ni(1)−O(1) and C(4)−Ni(1)−P(1) planes of 15.8° for **2**, 14.5° for **3**, and 14.8° for **4**, versus 4.3° for **1**. Examination of Table 1 shows other variations in metrical parameters without obvious trends. The additional steric bulk of the ligand backbone in compound **4** is transmitted throughout the structure in a way that hinders the rotation of the aryl ring bound to the carboxamide nitrogen and forces the ring to be more perpendicular relative to the coordination plane. This structural feature leads to a more effective blocking of the top and bottom of the square plane (pseudoaxial sites) by the ortho substituents.[14]

Table 1. Selected Bond Distances (Å) and Angles (deg)

	1	2	3	4	5
Ni(1)−N(2)	1.975(2)	1.975(3)	1.974(3)	1.984(2)	1.972(3)
Ni(1)−O(1)	1.910(2)	1.929(2)	1.903(2)	1.9016(18)	1.905(3)
Ni(1)−C(4)	1.926(2)	1.958(3)	1.946(4)	1.951(3)	1.945(4)
Ni(1)−P(1)	2.1483(8)	2.1535(10)	2.1521(12)	2.1395(10)	2.1513(12)
N(2)−Ni(1)−P(1)	169.9(6)	167.10(9)	166.01(9)	165.01(6)	170.05(11)
O(1)−Ni(1)−C(4)	175.53(0)	168.71(13)	169.21(14)	172.07(11)	175.45(16)
O(1)−Ni(1)−P(1)	87.35(5)	90.43(7)	87.98(8)	89.40(6)	87.95(9)
N(2)−Ni(1)−O(1)	82.63(7)	83.24(10)	82.43(11)	82.56(8)	82.79(13)
N(2)−Ni(1)−C(4)	96.27(10)	96.38(13)	97.55(14)	97.61(10)	96.75(15)
C(4)−Ni(1)−P(1)	93.79(8)	92.01(11)	93.77(12)	92.10(9)	92.76(12)
C(3)−N(1)−C(1)	116.4(2)	121.4(3)	116.3(3)	117.6(2)	118.4(3)
C(4)−Ni(1)−P(1)[a]	4.3	15.78(18)	14.45(20)	14.77(15)	5.89(0.21)

[a] Relative to N(2)−Ni(1)−O(1) plane.

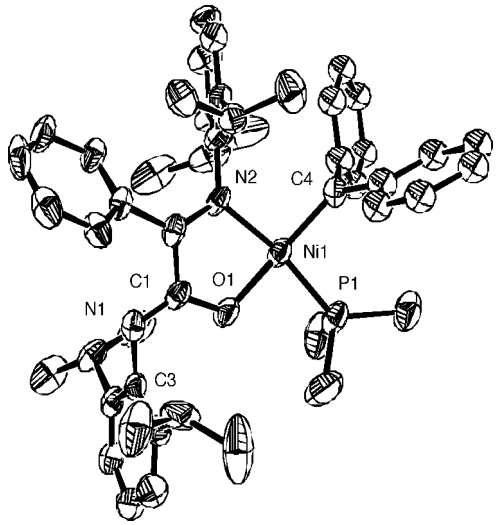

Figure 6. ORTEP drawing of **5** (R = Ph) at the 50% probability level showing both orientations of the phenyl ring on the benzyl ligand. Hydrogen atoms are omitted for clarity.

The ORTEP drawing of **5** is shown in Figure 6. Refined occupancy indicates that the disordered phenyl ring of the benzyl ligand is equally located in two orientations (49.7(3)%: 50.3(3)%). Compound **5** exhibits a smaller distortion from square-planar geometry with an N(2)−Ni(1)−P(1) angle of 170.05(11)° and an O(1)−Ni(1)−C(4) angle of 175.45(16)°. Bond angles and distances are in close agreement with those of **1**. The position of the phenyl substituent on the ligand backbone results in a less perpendicular arrangement between the square plane on Ni and the imine and carboxamide aryl rings. The result is that the ortho substituents are rotated away from the pseudoaxial sites, at least in the solid state.

Reactivity in Homopolymerization and Copolymerization Reactions. A series of ethylene homopolymerization and copolymerization reactions were carried out with the intent of examining how structural and electronic variations influence reactivity, and the results are summarized in Table 2. Ethylene homopolymerization reactions were performed using 10 μmoL of **1–7** and 25 μmoL of Ni(COD)$_2$ activator,[15] as illustrated in Scheme 3. Polymerizations were carried out using a 100 mL autoclave reactor in 30 mL of toluene at an ethylene pressure of 100 psi. The temperature was maintained at 20 °C over the course of the reaction.

(14) Schleis, T.; Spaniol, T.; Okuda, J.; Heinemann, J.; Mulhaupt, R. *J. Organomet. Chem.* **1998**, *569*, 159.

(15) See ref 6; the [Ni(COD)$_2$/[Ni-α-iminocarboxamide] ratio of 2.5 was determined in a previous study.

Comparison of entries 1–5 (Table 2) reveals an increase in monomer consumption activity as the bulk on the ligand framework increases, i.e., **1** < **2** ∼ **5** < **3** < **4**. A greater than 2-fold increase in activity is observed when the isopropyl derivative **4** is compared to the parent methyl species **1**. The M_n of the polymer products also increases proportionally with the increase in activity. Compound **4** exhibits the lowest molecular weight distribution (PDI ∼1.2) when compared to the other alkyl variants. The melting point of the polyethylene obtained is similar in all cases.

In the case of **5**, the activity and molecular weight observed are higher than those obtained with the parent species **1**. As shown in entries 5–7 of Table 2, the molecular weight and activity are higher for compound **6** and lower for **7** relative to **5**. This trend suggests that as electron density is removed from the metal center, the catalytic species becomes more active in ethylene polymerization reactions (i.e., reactivity: **6** > **5** > **7**). Polyethylene made with compounds **5–7** exhibit the narrowest polydispersities, between 1.1 and 1.2 in all cases. No discernible differences in the melting points of the polymer products were observed for compounds **5**−**7**.

Copolymerizations of ethylene and NBA were carried out using 20 μmoL of catalyst precursor and 50 μmoL of Ni(COD)$_2$ in a 0.15 M solution of NBA in 30 mL of toluene, as shown in Scheme 4. Ethylene was introduced and maintained at 100 psi and the reaction temperature was held at 20 °C. Examination of the products by ^{1}H NMR spectroscopy shows 1–13% molar NBA incorporation within the polyethylene backbone.

Focusing on compounds **1–5** (entries 8–13 in Table 2), one observes a trend in the rate of polymer production similar to that previously discussed for ethylene homopolymerizations. Compounds **1** and **2** exhibit roughly the same reactivity in copolymerization reactions in terms of activity and comonomer incorporation. Compound **3** stands out, as it leads to simultaneous high levels of activity and NBA enchainment with slightly broadened molecular weight distributions (entries 10 and 11). When compared to the parent compound **1**, similar copolymers are obtained in approximately half the time when using **3** (entry 10). Entry 11 shows that increasing the reaction time yields polymers with higher molecular weights and a decrease in the total comonomer content. The latter feature was previously used for the synthesis of tapered copolymer structures and reflects the fact that the monomer concentration is depleted as it becomes incorporated into the growing polymer chain.[7] When using **4** (entry 12), the NBA incorporation is substantially reduced compared to the other initiators. It is likely that the increased crowding around nickel substantially decreases the reactivity of the bulkier NBA, relative to ethylene.[16]

Copolymers made with **5** exhibit lower levels of incorporation than **1–3**; however, the molecular weight distribution remains

Table 2. Summary of Polymerization Reactions with 1–7

entry	precursor	comonomer	time [min]	activity [kg P/(mol Ni)(h)]	M_n [$\times 10^3$]	PDI	% inc.	T_m [°C]
1	**1**		20	220	80	1.3		127
2	**2**		20	255	86	1.3		127
3	**3**		20	420	121	1.4		129
4	**4**		20	534	182	1.2		128
5	**5**		20	259	102	1.2		127
6	**6**		20	280	113	1.1		127
7	**7**		20	180	91	1.2		126
8	**1**	NBA	30	109	68	1.4	13	62
9	**2**	NBA	30	105	65	1.3	13	57
10	**3**	NBA	15	177	63	1.5	12	76
11	**3**	NBA	30	176	97	1.6	7	96
12	**4**	NBA	30	243	186	1.3	1	118
13	**5**	NBA	30	141	92	1.2	7	68
14	**6**	NBA	30	104	75	1.3	7	68
15	**7**	NBA	30	157	83	1.3	5	72

Scheme 3. Polymerization of Ethylene Using 1–7 and $Ni(COD)_2$ as the Activator

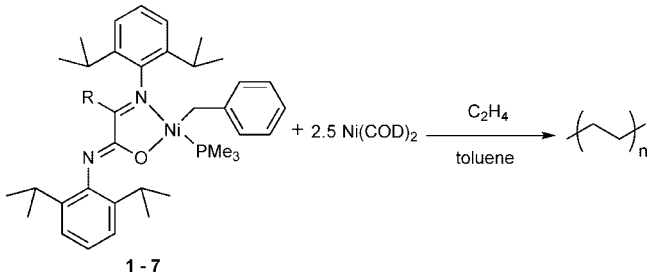

Scheme 4. Copolymerization of Ethylene and NBA Using 1–7 and $Ni(COD)_2$ as the Activator

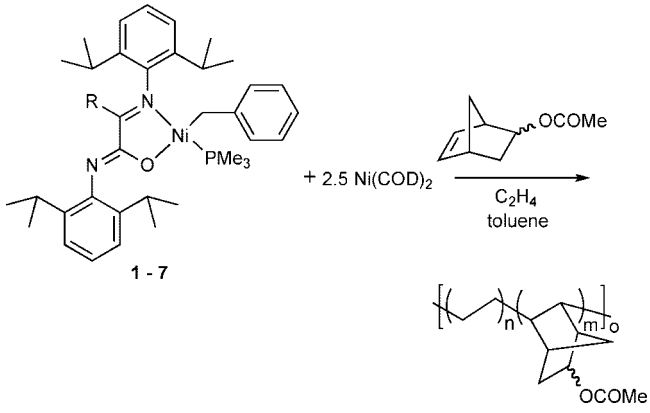

low over the course of the reaction (PDI ~1.2). Compound **6** exhibits the lowest overall activity in copolymerization reactions. When compared to **5**, this suggests that the more electron-deficient metal center interacts with the acetate functionality, potentially along the endo face of the comonomer, making enchainment less facile.[17] Compound **7** exhibits the highest activity relative to **5** and **6**; however, monomer incorporation is reduced.

Conclusions

The ability of α-iminocarboxamide nickel complexes to copolymerize functionalized norbornenes with ethylene under quasi-living polymerization characteristics facilitates the synthesis of polymers with unique properties and allows for the synthesis of more complex architectures. α-Iminocarboxamide ligands with sterically demanding alkyl substituents or aryl groups with different electronic properties at the site adjacent to the imine nitrogen can now be generated in a straightforward manner from the corresponding pyruvic acids via a method that utilizes $TiCl_4$. This methodology affords previously unattainable α-iminocarboxamide ligands that allow for an evaluation of how steric and electronic perturbations at the site adjacent to the imine functionality influence polymerization reactions.

Ethylene homopolymerization reactions show that as the bulk on the ligand framework increases, so does the monomer consumption activity and the molecular weight of the products, i.e., **1** < **2** < **3** < **4**. Additionally, as electron density is removed from the metal center, the catalytic species becomes more active in ethylene polymerization reactions. Copolymerizations with NBA illustrate that as the bulk on the backbone is increased, the reactivity of NBA relative to ethylene decreases. Compound **3**, however, exhibits high levels of activity and NBA enchainment, while compound **5** exhibits the most narrow molecular weight distribution in copolymerization reactions.

Experimental Section

General Remarks. All manipulations were performed under an inert atmosphere using standard glovebox and Schlenk-line techniques. Toluene and THF were distilled from sodium benzophenone ketyl, and pentane was distilled from Na/K alloy. The toluene for reactions with ethylene use was purchased from Aldrich (anhydrous grade) and further dried over Na/K alloy. 5-Norbornen-2-yl acetate was vacuum-distilled before use. Ethylene (99.99%) was purchased from Matheson Trigas and purified by passing through Agilent moisture and oxygen traps. Reagents, unless otherwise specified, were purchased from Aldrich and used without further purification. 2-Oxo-2-(4-(trifluoromethyl)phenyl)acetic acid and 2-(4-methoxyphenyl)-2-oxoacetic acid were purchased from Hansa Fine Chemicals and used as received. NMR spectra were obtained using Varian 400 and 500 spectrometers. ^1H and ^{13}C NMR spectra were calibrated using signals from the solvent. ^{31}P NMR and ^{19}F NMR spectra were calibrated and reported downfield from an external H_3PO_4 standard and α,α,α-trifluorotoluene in [d_6]-benzene respectively. Polymerization activities were calculated from the mass of the product obtained. Polymers were characterized by GPC analysis, relative to polystyrene standards, at 135 °C in *o*-dichlorobenzene (in a Polymer Laboratories, high-temperature chromatograph, PL-GPC 200). Polymer melting points were measured on a TA Instruments differential scanning calorimeter (model DSC 2920) at a rate of 10 °C/min for three cycles using a temperature range

(16) Benedikt, G. M.; Elce, E.; Goodall, B. L.; Kalamarides, H. A.; McIntosh, L. H.; Rhodes, L. F.; Selvy, K. T.; Andes, C.; Oyler, K.; Sen, A. *Macromolecules* **2002**, *35*, 8978.

(17) Hennis, A. D.; Polly, J. D.; Long, G. S.; Sen, A.; Yandulov, D.; Lipian, D.; Benedikt, G. M.; Rhodes, L. F.; Huffman, J. *Organometallics* **2001**, *20*, 2802.

Table 3. Crystal Data and Structure Refinement for Compounds 2–5

	2	3	4	5
empirical formula	C_{38} H_{55} N_2 NiOP	C_{40} H_{59} N_2NiOP	C_{39} H_{57} N_2NiOP	$C_{42}H_{55}$ N_2 NiOP
fw	645.52	673.57	659.55	693.56
temp (K)	150(2)	140(2)	150(2)	150(2)
wavelength (Å)	0.71073	0.71073	0.71073	0.71073
cryst syst	monoclinic	monoclinic	monoclinic	monoclinic
space group	$P2_1/n$	$P2_1/c$	$P2_1/c$	$P2_1/n$
unit-cell dimens (Å, deg)	a = 10.1616(14)	a = 10.2237(16)	a = 9.716(3)	a = 9.9429(7)
	b =36.813(5)	b = 21.053(3)	b = 20.040(7)	b = 25.4501(19)
	c = 20.361(3)	c = 18.063(3)	c = 19.496(6)	c = 15.2227(11)
	α = 90	α = 90	α = 90	α = 90
	β = 92.918(2)	β = 96.135(3)	β =100.578(5)	β = 93.662(2)
	γ = 90	γ = 90	γ = 90	γ = 90
volume (Å^3)	7606.6(18)	3865.7(11)	3732(2)	3844.2(5)
Z	8	4	4	4
density (calcd) Mg/m^3	1.127	1.157	1.174	1.198
absorp coeff (mm^{-1})	0.581	0.574	0.593	0.579
F(000)	2784	1456	1424	1488
cryst size (mm^3)	0.35 × 0.3 × 0.1	0.2x 0.16x 0.08	0.3x 0.2 × 0.2	0.2x 0.15x 0.15
θ range (deg)	1.11 to 26.67	1.49 to 26.43	1.47 to 27.54	2.09 to 26.37
index ranges	$-12 \le h \le 12$	$-12 \le h \le 11$	$-11 \le h \le 12$	$-12 \le h \le 12$
	$-45 \le k \le 46$	$-26 \le k \le 26$	$-25 \le k \le 24$	$-31 \le k \le 31$
	$-25 \le l \le 24$	$-22 \le l \le 22$	$-25 \le l \le 25$	$-19 \le l \le 19$
no. of reflns collected	60 496	30 577	28 366	31 209
no. of indep reflns	15 412 [R(int) = 0.0754]	7787 [R(int) = 0.1071]	7841 [R(int) = 0.0506]	7759 [R(int) = 0.0695]
completeness to the respective θ	96.0	97.8	91.1	98.6
no. of data/restraints/params	15 412/ 6/831	7787/5/439	7841/0/430	7759/12/435
goodness-of-fit on F^2	0.897	0.832	0.871	1.451
final R indices [$I > 2\sigma(I)$][a]	R1 = 0.0586, wR2 = 0.1296	R1 = 0.0548, wR2 = 0.1066	R1 = 0.0492, wR2 = 0.1120	R1 = 0.0682, wR2 = 0.1465
R indices (all data)	R1 = 0.1153, wR2 = 0.1551	R1 = 0.1340, wR2 = 0.1277	R1 = 0.0810, wR2 = 0.1194	R1 = 0.1315, wR2 = 0.1573
largest diff peak and hole (e Å^{-3})	1.019 and −0.475	0.511 and −0.331	1.233 and −0.268	1.057 and −0.360

[a] Definitions: R1 = $\sum||F_o| - |F_c||/\sum|F_o|$, wR2 = $[\sum(F_o^2 - F_c^2)^2]/\sum[w(F_o^2)^2]]^{1/2}$, GOF = $[\sum[w(F_o^2 - F_c^2)^2]/(n - p)]^{1/2}$, where n is the number of reflections and p is the total number of refined parameters. * min./max.

of 0–180 °C. ^{1}H NMR spectra of the polymers were obtained in 1,1,2,2-tetrachloroethane-d_2 at 115 °C. Elemental analyses were performed by Analytic Laboratory, Marine Science Institute, University of California, Santa Barbara. Gas chromatography/mass spectroscopy was carried out on a Shimadzu GC-17A gas chromatograph and Shimadzu GCMS-QP5000 gas chromatograph–mass spectrometer.

X-ray Crystallography. The monocrystal was mounted on a glass fiber and transferred to a Bruker CCD platform diffractometer. The SMART[18] program package was used to determine the unit-cell parameters and for data collection (25 s/frame scan time for a sphere of diffraction data). The raw frame data were processed using SAINT[19] and SADABS[20] to yield the reflection data file. Subsequent calculations were carried out using the SHELXTL[21] program. The structure was solved by direct methods and refined on F^2 by full-matrix least-squares techniques. Analytical scattering factors for neutral atoms were used throughout the analysis.[22] Hydrogen atoms were located from a difference Fourier map and refined (x,y,z and U_{iso}).[23] Single crystals of **2**–**5** suitable for X-ray diffraction studies were obtained by slow crystallization from pentane. The crystal data and refinement are summarized in Table 3.

Synthesis and Characterization of Compounds. Typical Reaction Using $TiCl_4$. Included here are representative procedures. Complete details are available in the Supporting Information.

***N*-(2,6-Diisopropylphenyl)-2-(2,6-diisopropylphenylimino)-2-phenylethanamide.** In the glovebox, a dry solution of 2,6-diisopropylaniline (572 mg, 3.23 mmol) and triethylamine (2.94 g, 29.1 mmol) in toluene (90 mL) was chilled to −35 °C. Titanium tetrachloride (673 mg, 3.55 mmol) in 10 mL of toluene was added dropwise over a period of 5 min to give a deep red solution, which was allowed to stir for an additional 10 min. A chilled solution of *N*-(2,6-diisopropylphenyl)-2-oxo-2-phenylethanamide in 10 mL of toluene (1.00 g, 3.23 mmol) was added at once. The solution was vigorously stirred, allowed to warm to room temperature, and stirred overnight. Subsequently, 250 mL of diethyl ether was added, and the resulting suspension was stirred overnight open to air. The suspension was filtered through a silica plug, and removal of the solvent gave 1.39 g (2.97 mmol) of the desired product (92.0%). ^{1}H NMR (399.95 MHz, [d_1]-chloroform, 298 K): δ 9.22 (br, 1 H, N-*H*), 7.35 (t, $^3J_{HH}$ = 7.1 Hz, 1 H, ph-H), 7.30–7.21 (m, 7 H, ph-H), 7.10 (m, 3 H, ph-H), 3.26 (septet, $^3J_{HH}$ = 6.8 Hz, 2 H, *i*Pr-C*H*), 2.80 (septet, $^3J_{HH}$ = 6.8 Hz, 2 H, *i*Pr-C*H*), 1.30 (d, $^3J_{HH}$ = 6.8 Hz, 12 H, *i*Pr-CH_3), 1.18 (d, $^3J_{HH}$ = 6.8 Hz, 6 H, *i*Pr-CH_3), 0.93 (d, $^3J_{HH}$ = 6.8 Hz, 6 H, *i*Pr-CH_3). ^{13}C NMR (125.7 MHz, [d_1]-chloroform, 298 K): 162.64, 159.94 (carbonyl and imine), 145.95, 143.67, 135.24, 131.38, 130.14, 129.84, 128.29, 127.68, 124.80, 123.49, 123.19 (ph-C), 29.19, 28.67 (*i*Pr-CH), 23.70, 23.52, 21.82 (*i*Pr-CH_3). Anal. Calcd ($C_{32}H_{40}N_2O$): C, 82.01; H, 8.60; N, 5.98. Found: C, 81.83; H, 8.55; N, 5.97.

***N*-(2,6-Diisopropylphenyl)-2-(2,6-diisopropylphenylimino)-3-methylbutanamide.** In the glovebox, a dry solution of 2,6-diisopropylaniline (964 mg, 5.45 mmol) and triethylamine (4.95 g, 49.0 mmol) in toluene (100 mL) was chilled to −35 °C. Titanium tetrachloride (1.03 g, 5.45 mmol) in 10 mL of toluene was added dropwise over a period of 5 min to give a deep red solution, which was allowed to stir for an additional 10 min. A chilled solution of *N*-(2,6-diisopropylphenyl)-3-methyl-2-oxo-2-butanamide in 25 mL of toluene (1.5 g, 5.45 mmol) was added at once. The solution was heated, under nitrogen, to 85 °C and allowed to stir overnight. The solution was opened to the atmosphere, allowed to cool, and added to 250 mL of diethyl ether. Stirring overnight gave a yellow suspension. Filtration through Celite followed by column chromatography on silica gel using hexane and ether (v/v, 4:1) gave 1.68 g

(18) *SMART Software Users Guide, Version 5.1*; Bruker Analytical X-Ray Systems, Inc.; Madison, WI1999.
(19) *SAINT Software Users Guide, Version 6.0*; Bruker Analytical X-Ray Systems, Inc.: Madison, WI, 1999.
(20) Sheldrick, G. M. *SADABS, Version 2.05*; Bruker Analytical X-Ray Systems, Inc.: Madison, WI, 2001.
(21) Sheldrick, G. M. *SHELXTL Version 6.12*; Bruker Analytical X-Ray Systems, Inc.: Madison, WI, 2001.
(22) *International Tables for X-Ray Crystallography*; Kluwer Academic Publishers: Dordrecht, 1992; Vol. C.
(23) Flack, H. D. *Acta Crystallogr.* **1983**, *A39*, 876.

of the product (71.0%). ^{1}H NMR (399.95 MHz, [d_1]-chloroform, 298 K): δ 8.90 (br, 1 H, N-*H*), 7.30 (t, $^3J_{HH}$ = 8.0 Hz, 1 H, ph-H^4), 7.26 (d, $^3J_{HH}$ = 8.6 Hz, 2 H, ph-H^{3,5}), 7.20–7.09 (m, 3 H, ph-H), 3.13 (septet, $^3J_{HH}$ = 6.8 Hz, 2 H, *i*Pr-C*H*), 2.72 (septet, $^3J_{HH}$ = 6.8 Hz, 2 H, *i*Pr-C*H*), 2.63 (septet, $^3J_{HH}$ = 6.8 Hz, 1 H, *i*Pr-C*H*), 1.29 (d, $^3J_{HH}$ = 6.8 Hz, 6 H, *i*Pr-CH_3), 1.28 (d, $^3J_{HH}$ = 5.5 Hz, 6 H, *i*Pr-CH_3), 1.24 (d, $^3J_{HH}$ = 6.8 Hz, 6 H, *i*Pr-CH_3), 1.15 (d, $^3J_{HH}$ = 6.8 Hz, 6 H, *i*Pr-CH_3), 1.10 (t, $^3J_{HH}$ = 7.7 Hz, 3 H CH_3). ^{13}C NMR (125.7 MHz, [d_1]-chloroform, 298 K): δ 169.16, 161.82 (carbonyl and imine), 145.86 (amide-ph-C), 143.70 (imine-ph-C), 134.99 (imine-ph-C), 131.23 (amide-ph-C), 128.10 (amide-ph-C), 124.34 (imine-ph-C), 123.40, 122.92 (ph-C), 31.34, 29.10, 28.34 (*i*Pr-CH), 23.55, 23.42, 21.94, 18.90 (*i*Pr-CH_3). Anal. Calcd ($C_{28}H_{40}N_2O$): C, 80.13; H, 9.74; N, 6.44. Found: C, 79.88; H, 9.80; N, 6.47.

[*N*-(2,6-Diisopropylphenyl)-2-(2,6-diisopropylphenylimino)-butanamidato-κ^2N,O](η^1-CH$_2$Ph) (PMe$_3$)nickel (2). Potassium *N*-(2,6-diisopropylphenyl)-2-(2,6-diisopropylphenylimino)butanamidate (100 mg, 0.218 mmol) in toluene was added to Ni(η^1-CH$_2$Ph)Cl(PMe$_3$)$_2$ (73.6 mg, 0.218 mmol), and the mixture was stirred for 2.5 h at room temperature. The suspension was filtered, and all volatiles were removed under vacuum to give a red solid. Crystallization from pentane at −35 °C overnight gave the product as a dark orange solid (115.5 mg, 0.179 mmol, 82.1% yield). Single crystals for X-ray crystallography were grown by slow recrystallization from pentane at −35 °C. ^{1}H NMR (399.95 MHz, [d_6]-benzene, 298 K): δ 7.69 – 7.67 (m, 2 H, ph-H), 7.42 (d, $^3J_{HH}$ = 7.7 Hz, 2 H, ph-H), 7.35 (t, $^3J_{HH}$ = 8.0 Hz, 1 H, ph-H), 7.19–7.05 (m, 6 H, ph-H), 3.72 (septet, $^3J_{HH}$ = 6.8 Hz, 2 H, *i*Pr-C*H*), 3.64 (septet, $^3J_{HH}$ = 6.8 Hz, 2 H, *i*Pr-C*H*), 2.67 (quartet, $^3J_{HH}$ = 7.4 Hz, 2 H, Et-CH_2), 1.60 (br, 12 H, *i*Pr-CH_3), 1.50 (d, $^3J_{HH}$ = 7.4, 3 H, CH_3), 1.48 (d, $^3J_{HH}$ = 6.5 Hz, 6 H, *i*Pr-CH_3), 1.30 (d, $^3J_{HH}$ = 7.1 Hz, 6 H, *i*Pr-CH_3), 1.14 (br s, 2 H, benzyl-CH_2), 0.55 (d, $^2J_{HP}$ = 10.4, 9 H, PCH_3). ^{13}C NMR (125.7 MHz, [d_6]-benzene, 298 K): δ 184.79 (carbonyl), 163.94, 150.80, 147.37, 141.03, 140.30, 138.30, 129.81, 127.29, 124.04, 123.53, 122.55, 122.40 (imine and ph-C), 29.43, 28.64 (*i*Pr-CH), 26.67, 24.37, 24.12 (*i*Pr-CH_3), 23.79 (Et-CH_2), 11.94 (d, $^1J_{CP}$ = 27 Hz, P*C*H$_3$) 9.41 (d, $^2J_{CP}$ = 31 Hz, *C*H$_2$Ph). ^{31}P NMR (161.19 MHz, [d_6]-benzene, 298 K, H_3PO_4): δ −8.01 ppm. Anal. Calcd ($C_{38}H_{55}N_2NiOP$): C, 70.70; H, 8.59; N, 4.34. Found: C, 70.60; H, 8.54; N, 4.32.

[*N*-(2,6-Diisopropylphenyl)-2-(2,6-diisopropylphenylimino)-4-methylpentanamidato-κ^2N,O](η^1-CH$_2$Ph)(PMe$_3$)nickel (3). Potassium *N*-(2,6-diisopropylphenyl)-2-(2,6-diisopropylphenylimino)-4-methylpentanamidate (180.7 mg, 0.371 mmol) was added to Ni(η^1-CH$_2$Ph)Cl(PMe$_3$)$_2$ (125.2 mg, 0.371 mol), and the mixture was stirred for 2.5 h at room temperature. The suspension was filtered, and all volatiles were removed under vacuum to give a red solid. Crystallization from pentane at −35 °C overnight gave the product as a dark orange solid (225.7 mg, 0.335 mmol) in 90.3% yield. Single crystals for X-ray crystallography were grown by slow crystallization from pentane. ^{1}H NMR (399.95 MHz, [d_6]-benzene, 298 K): δ 7.77–7.75 (m, 2 H, ph-H), 7.42 (d, $^3J_{HH}$ = 7.4 Hz, 2 H, ph-H), 7.31–7.05 (m, 7 H, ph-H), 3.78–3.64 (m, 4 H, *i*Pr-C*H*), 2.92–2.82 (m, 3 H, *i*But-C*H*), 1.77–1.62 (br s, 6H,*i*Pr-CH_3), 1.62–1.54 (br s, 6 H, *i*Pr-CH_3), 1.53 (d, $^3J_{HH}$ = 6.8 Hz, 6 H, *i*Pr-CH_3), 1.41 (d, $^3J_{HH}$ = 6.8, 6 H, *i*Pr-CH_3), 1.10 (br d, $^3J_{HH}$ = 3.4 Hz, 2 H, benzyl-CH_2), 1.06 (d, $^3J_{HH}$ = 6.5, 6 H, *i*But-CH_3), 0.52 (d, $^2J_{HP}$ = 10.1, 9 H, PCH_3). ^{13}C NMR (125.7 MHz, [d_6]-benzene, 298 K): δ 184.24 (carbonyl), 164.97, 150.65, 147.47, 140.94, 140.30, 138.39, 129.96, 127.47, 124.22, 123.62, 122.55, 122.43, 41.57 (imine and ph-C), 29.46, 28.61 (*i*Pr-CH), 27.22, 25.15, 24.06 (*i*Pr-CH_3), 23.79, 23.182 (*i*But-*C*H$_2$ and *C*H$_3$), 11.82 (d, $^1J_{CP}$ = 27 Hz, P*C*H$_3$) 9.65 (d, $^2J_{CP}$ = 31 Hz, *C*H$_2$Ph). ^{31}P NMR (161.19 MHz, [d_6]-benzene, 298 K, H_3PO_4): δ −7.85 ppm. Anal. Calcd ($C_{40}H_{59}N_2NiOP$): C, 71.32; H, 8.83; N, 4.16. Found: C, 71.15; H, 8.63; N, 4.15.

[*N*-(2,6-Diisopropylphenyl)-2-(2,6-diisopropylphenylimino)-3-methylbutanamidato-κ^2N,O](η^1-CH$_2$Ph)(PMe$_3$)nickel (4). Potassium *N*-(2,6-diisopropylphenyl)-2-(2,6-diisopropylphenylimino)-3-methylbutanamidate (100 mg, 0.211 mmol) in toluene was added to Ni(η^1-CH$_2$Ph)Cl(PMe$_3$)$_2$ (71.2 mg, 0.211 mmol), and the mixture was stirred for 2.5 h at room temperature. The suspension was filtered, and all volatiles were removed under vacuum to give a red solid. Successive recrystallizations from pentane at −35 °C overnight gave the product as an orange solid (114.2 mg, 0.182 mmol, 86.0% yield). Single crystals for X-ray crystallography were grown by slow recrystallization from pentane at −35 °C. ^{1}H NMR (399.95 MHz, [d_6]-benzene, 298 K): δ 7.74 – 7.68 (m, 2 H, ph-H), 7.41 (d, $^3J_{HH}$ = 7.7 Hz, 2 H, ph-H), 7.31–7.27 (m, $^3J_{HH}$ = 8.0 Hz, 2 H, ph-H), 7.14–7.06 (m, 5 H, ph-H), 3.66 – 3.56 (m, 4 H, *i*Pr-C*H*), 2.87 (septet, *J* = 6.8 Hz, 1 H, *i*Pr-C*H*), 1.73 (d, $^3J_{HH}$ = 6.8, 6H, *i*Pr-CH_3), 1.63 (d, $^3J_{HH}$ = 7.1 Hz, 6 H, *i*Pr-CH_3), 1.57 (d, $^3J_{HH}$ = 6.8 Hz, 6 H, *i*Pr-CH_3), 1.54 (d, $^3J_{HH}$ = 7.06 Hz, 6 H, *i*Pr-CH_3), 1.37 (d, $^3J_{HH}$ = 6.8 Hz, 6 H, *i*Pr-CH_3), 1.06 (br s, 2 H, benzyl-CH_2), 0.53 (d, $^2J_{HP}$ = 10.4, 9 H, PCH_3). ^{13}C NMR (125.7 MHz, [d_6]-benzene, 298 K): δ 186.18 (carbonyl), 163.70, 150.95, 147.56, 141.28, 140.09, 138.12, 129.84, 127.20, 124.16, 123.49, 122.43, 122.34 (imine and ph-C), 33.32, 29.34, 28.40 (*i*Pr-CH), 24.85, 24.30, 23.91, 23.76, 20.57 (*i*Pr-CH_3), 11.84 (d, $^1J_{CP}$ = 27 Hz, P*C*H$_3$), 9.92 (d, $^2J_{CP}$ = 31 Hz, *C*H$_2$Ph). ^{31}P NMR (161.19 MHz, [d_6]-benzene, 298 K, H_3PO_4): δ −8.00 ppm. Anal. Calcd ($C_{38}H_{55}N_2NiOP$): C, 71.02; H, 8.71; N, 4.25. Found: C, 70.97; H, 8.59; N, 4.24.

[*N*-(2,6-Diisopropylphenyl)-2-(2,6-diisopropylphenylimino)-2-phenylethanamidato-κ^2N,O](η^1-CH$_2$Ph)(PMe$_3$)nickel (5). Potassium *N*-(2,6-diisopropylphenyl)-2-(2,6-diisopropylphenylimino)-2-phenylethanamideate (272 mg, 0.537 mmol) was added to Ni(η^1-CH$_2$Ph)Cl(PMe$_3$)$_2$ (178.6 mg, 0.529 mmol), and the mixture was stirred for 2.5 h at room temperature. The suspension was filtered, and all volatiles were removed under vacuum to give a red solid. Crystallization from pentane at −35 °C overnight gave the product (227.5 mg, 0.328 mmol) as a dark red crystalline solid in 61.1% yield. Single crystals for X-ray crystallography were grown by slow recrystallization from pentane at −35 °C. ^{1}H NMR (399.95 MHz, [d_6]-benzene, 298 K): δ 7.80– 7.75 (m, 4 H, ph-H), 7.43 (d, $^3J_{HH}$ = 7.4 Hz, 2 H, ph-H), 7.33–7.30 (m, 2 H, ph-H), 7.23–7.02 (m, 8 H, ph-H), 4.19 (septet, $^3J_{HH}$ = 6.8 Hz, 2 H, *i*Pr-C*H*), 3.59 (septet, $^3J_{HH}$ = 6.8 Hz, 2 H, *i*Pr-C*H*), 1.74–1.53 (br, 12 H, *i*Pr-CH_3), 1.49 (d, $^3J_{HH}$ = 6.8, 6 H, CH_3), 1.25 (s, 2 H, benzyl-CH_2), 1.10 (d, $^3J_{HH}$ = 6.8 Hz, 6 H, *i*Pr-CH_3), 0.64 (d, $^2J_{HP}$ = 10.1 Hz, 9 H, PCH_3). ^{13}C NMR (125.7 MHz, [d_6]-benzene, 298 K): δ 176.44 (carbonyl), 165.46, 150.71, 147.80, 141.06, 140.34, 137.79, 134.08, 130.69, 129.86, 129.78, 127.89, 127.50, 127.23, 124.10, 123.53, 122.49, 122.37 (imine and ph-C), 29.43, 29.10 (*i*Pr-CH), 24.58, 23.73, 23.49 (*i*Pr-CH_3), 11.94 (d, $^1J_{CP}$ = 27 Hz, P*C*H$_3$), 10.03 (d, $^2J_{CP}$ = 27 Hz, *C*H$_2$Ph). ^{31}P NMR (161.19 MHz, [d_6]-benzene, 298 K, H_3PO_4): δ −8.03 ppm. Anal. Calcd ($C_{42}H_{55}N_2NiOP$): C, 72.73; H, 7.99; N, 4.04. Found: C 72.56; H, 7.90; N, 3.99.

[*N*-(2,6-Diisopropylphenyl)-2-(2,6-diisopropylphenylimino)-2-(4-(trifluoromethyl)phenyl)acetamidato-κ^2N,O](η^1-CH$_2$Ph)-(PMe$_3$)nickel (6). Potassium *N*-(2,6-diisopropylphenyl)-2-(2,6-diisopropylphenylimino)-2-(4-(trifluoromethyl)phenyl)acetamidate (100 mg, 0.174 mmol) was added to Ni(η^1-CH$_2$Ph)Cl(PMe$_3$)$_2$ (58.7 mg, 0.174 mmol), and the mixture was stirred for 2.5 h at room temperature. The suspension was filtered, and all volatiles were removed under vacuum to give a red solid. Crystallization from pentane at −35 °C overnight gave the product (109 mg, 0.143 mmol) as a dark red crystalline solid in 82.2% yield. ^{1}H NMR (399.95 MHz, [d_6]-benzene, 298 K): δ 7.62– 7.60 (m, 4 H, ph-H), 7.27 (d, $^3J_{HH}$ = 7.4 Hz, 2 H, ph-H), 7.18–7.13 (m, 3 H, ph-H), 7.04–6.93 (m, 6 H, ph-H), 3.95 (septet, $^3J_{HH}$ = 6.8 Hz, 2 H, *i*Pr-C*H*), 3.38 (septet, $^3J_{HH}$ = 7.1 Hz, 2 H, *i*Pr-C*H*), 1.60–1.36 (br, 12 H, *i*Pr-CH_3), 1.31 (d, $^3J_{HH}$ = 6.8, 6 H, CH_3), 1.08 (s, 2 H, benzyl-

CH_2), 0.88 (d, $^3J_{HH}$ = 7.1 Hz, 6 H, *i*Pr-CH_3), 0.48 (d, $^2J_{HP}$ = 10.4 Hz, 9 H, PCH_3). ^{13}C NMR (125.7 MHz, [d_6]-benzene, 298 K): δ 175.08 (carbonyl), 165.12, 150.29, 147.34, 140.52, 140.12, 137.73, 137.36, 130.87, 129.72, 127.89, 124.25, 123.71, 122.77, 122.46 (imine and ph-C), 29.46, 29.04 (*i*Pr-CH), 24.55, 23.70, 23.27 (*i*Pr-CH_3), 11.89 (d, $^1J_{CP}$ = 24 Hz, PCH_3), 10.03 (d, $^2J_{CP}$ = 27 Hz, CH_2Ph). ^{31}P NMR (161.19 MHz, [d_6]-benzene, 298 K, H_3PO_4): δ −8.05 ppm. ^{19}F NMR (161.19 MHz, [d_6]-benzene, 298 K, α,α,α-trifluorotoluene): δ −0.26 ppm. Anal. Calcd ($C_{43}H_{54}F_3N_2NiOP$): C, 67.82; H, 7.15; N, 3.68. Found: C, 67.38; H, 7.09; N, 3.69.

***N*-(2,6-Diisopropylphenyl)-2-(2,6-diisopropylphenylimino)-2-(4-(methoxyphenyl)acetamidato-κ^2N,O](η^1-CH$_2$Ph)-(PMe$_3$)nickel (7).** Potassium *N*-(2,6-diisopropylphenyl)-2-(2,6-diisopropylphenylimino)-2-(4-(methoxyphenyl)acetamidate (100 mg, 0.186 mmol) was added to Ni(η^1-CH_2Ph)Cl(PMe_3)$_2$ (62.8 mg, 0.186 mmol), and the mixture was stirred for 2.5 h at room temperature. The suspension was filtered, and all volatiles were removed under vacuum to give a red solid. Crystallization from pentane at −35 °C over the course of two days gave the product (106 mg, 0.146 mmol) as a dark red solid in 78.8% yield. ^{1}H NMR (399.95 MHz, [d_6]-benzene, 298 K): δ 7.78 (d, $^3J_{HH}$ = 8.9 Hz, 2 H, ph-H), 7.72 (d, $^3J_{HH}$ = 7.7 Hz, 2 H, ph-H), 7.40 (d, $^3J_{HH}$ = 7.7 Hz, 2 H, ph-H), 7.30–7.26 (m, 2 H, ph-H), 7.22–7.05 (m, 5 H, ph-H), 6.68 (d, $^3J_{HH}$ = 8.9 Hz, 2 H, ph-H), 4.18 (septet, $^3J_{HH}$ = 6.8 Hz, 2 H, *i*Pr-CH), 3.60 (septet, $^3J_{HH}$ = 6.8 Hz, 2 H, *i*Pr-CH), 1.72–1.57 (br, 6 H, *i*Pr-CH_3), 1.46 (d, $^3J_{HH}$ = 6.8, 12 H, CH_3), 1.21 (s, 2 H, benzyl-CH_2), 1.12 (d, $^3J_{HH}$ = 7.1 Hz, 6 H, *i*Pr-CH_3), 0.61 (d, $^2J_{HP}$ = 10.4 Hz, 9 H, PCH_3). ^{13}C NMR (125.7 MHz, [d_6]-benzene, 298 K): δ 175.65 (carbonyl), 165.73, 161.27, 150.92, 148.01, 141.55, 140.43, 137.87, 133.20, 129.86, 129.81, 129.78, 127.37, 126.98, 126.29, 124.22, 123.46, 122.40, 122.37, 112.78 (imine and ph-C), 54.59, 29.43, 29.10 (*i*Pr-CH), 24.49, 23.82, 23.64, 14.26 (*i*Pr-CH_3), 12.00 (d, J = 27 Hz, PCH_3), 10.12 (d, $^2J_{CP}$ = 34 Hz, CH_2Ph). ^{31}P NMR (161.19 MHz, [d_6]-benzene, 298 K, H_3PO_4): δ −8.06 ppm. Anal. Calcd ($C_{43}H_{57}N_2NiOP$): C, 71.37; H, 7.94; N, 3.87. Found: C, 70.80; H, 7.82; N, 3.87.

Typical Reaction with Ethylene. Polymerizations were conducted in the following manner using the initiators **1**–**7**. An autoclave reactor (100 mL) was loaded inside a glovebox with an appropriate amount (10 μmol) of the α-iminocarboxamide complex and (25 μmol) Ni(COD)$_2$ and toluene, such that the final volume of the toluene solution was 30 mL. The reactor was sealed inside the glovebox and attached to an ethylene line. Ethylene was fed into the reactor continuously at 100 psi, and the pressurized reaction mixture was stirred at 20 °C. Ethylene was vented after 20 min, and acetone was added to quench the polymerization. The precipitated polymer was collected by filtration and dried under high vacuum overnight.

Typical Reaction with Ethylene and 5-Norbornen-2-yl acetate (NBA). An autoclave reactor (100 mL) was loaded inside a glovebox with an α-iminocarboxamide complex (20 μmol) and Ni(COD)$_2$ (50 μmol), 5-norbornen-2-yl acetate (4.50 mmol), and toluene, such that the final volume of the toluene solution was 30 mL. The reactor was sealed inside the glovebox and attached to an ethylene line. Ethylene was fed into the reactor continuously at 100 psi, and the pressurized reaction mixture was stirred at 20 °C. Ethylene was vented after a specified amount of time, and acetone added to quench the polymerization. The precipitated polymer was collected by filtration and dried under high vacuum overnight.

Acknowledgment. This work was funded through the Mitsubishi Chemical Center for Advanced Materials and the Department of Energy. The authors are grateful to Prof. Rene S. Rojas and Dr. Jacek Brzezinski for useful discussions.

Supporting Information Available: Complete details for the synthesis and characterization of all compounds. This material is available free of charge via the Internet at http://pubs.acs.org.

OM8000263